Supplementary Information

Boosted mechanosensitivity of stretchable conductive composite strain sensors based on kirigami cut design

Sung-Hun Ha [a] and Jong-Man Kim *[a,b]

[a] Department of Nano Fusion Technology, Pusan National University, Busan 46214, Republic of Korea.

[b]Department of Nanoenergy Engineering and Research Center for Energy Convergence Technology, Pusan National University, Busan 46214, Republic of Korea.

*Corresponding author: jongkim@pusan.ac.kr

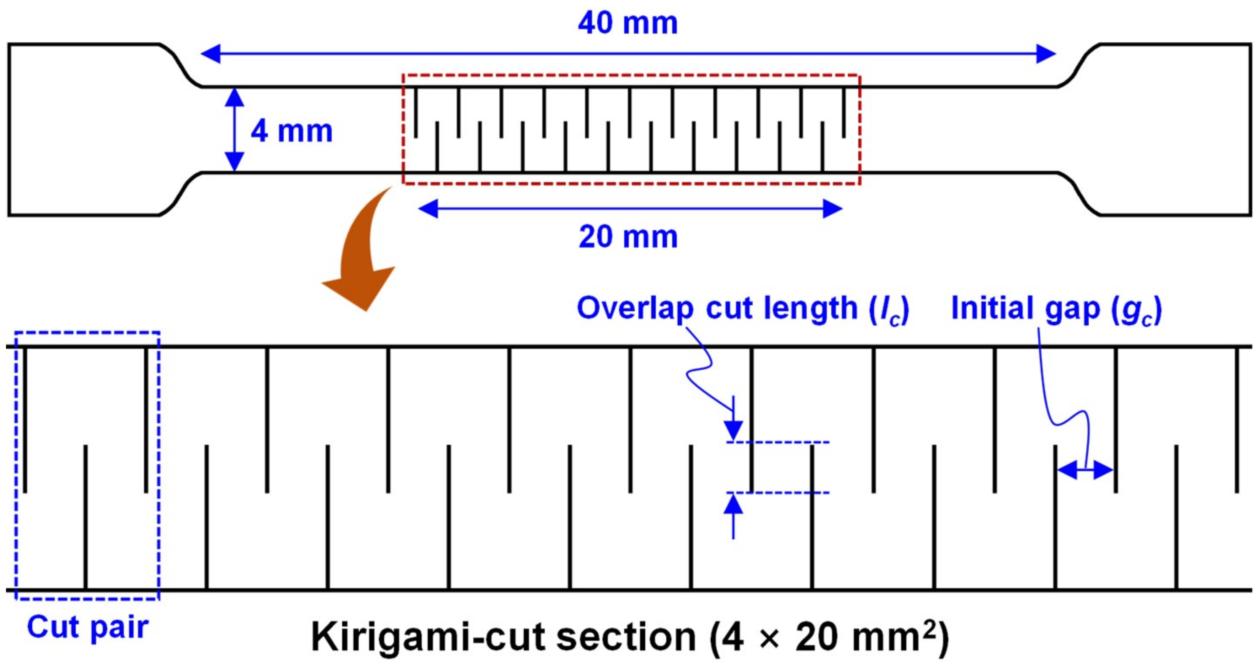

Fig. S1 Detailed layout of the kirigami-cut section in the designed CUT strain sensor.

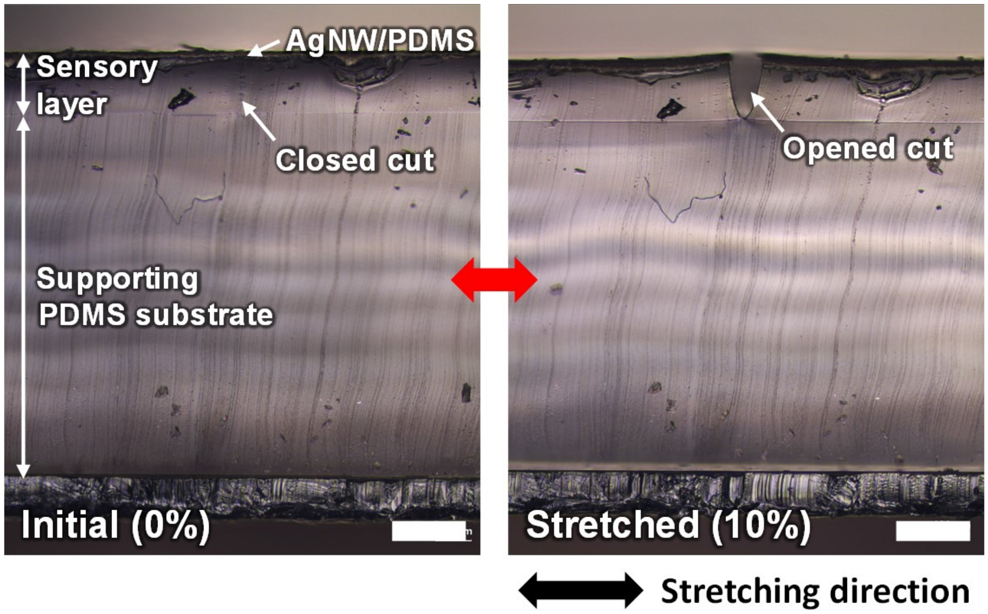

Fig. S2 Cross-sectional microscope images of the CUT-10 sensor in the initial and 10%-stretched states (scale bars: 200 μm).

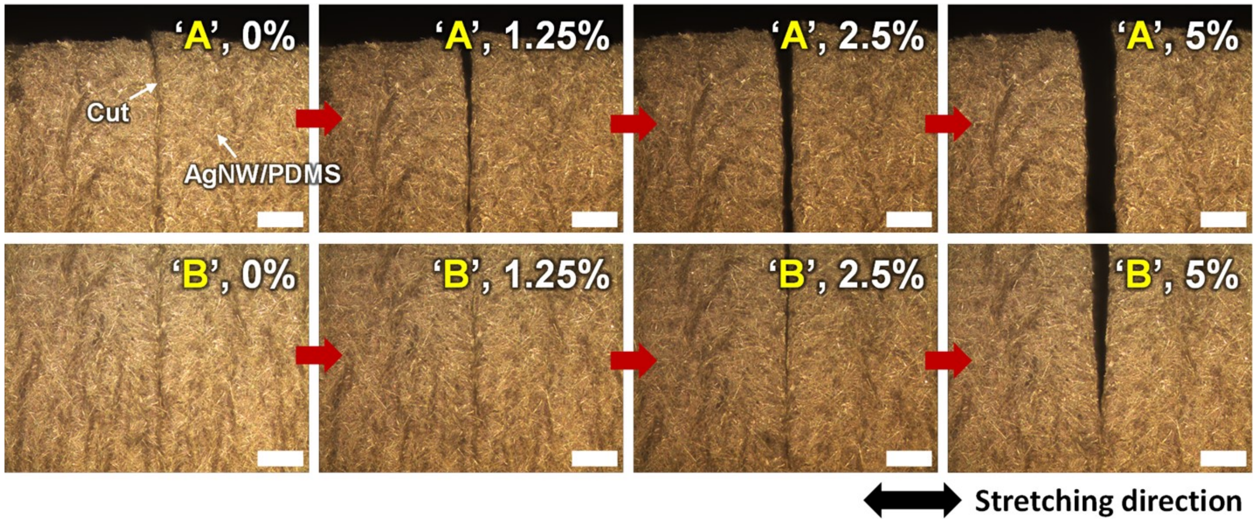

Fig. S3 Sequential microscope images showing the detailed strain-dependent opening process of mechanical cuts of the CUT strain sensor (CUT-10 model) in the first stretching phase (scale bars: 200 μm).

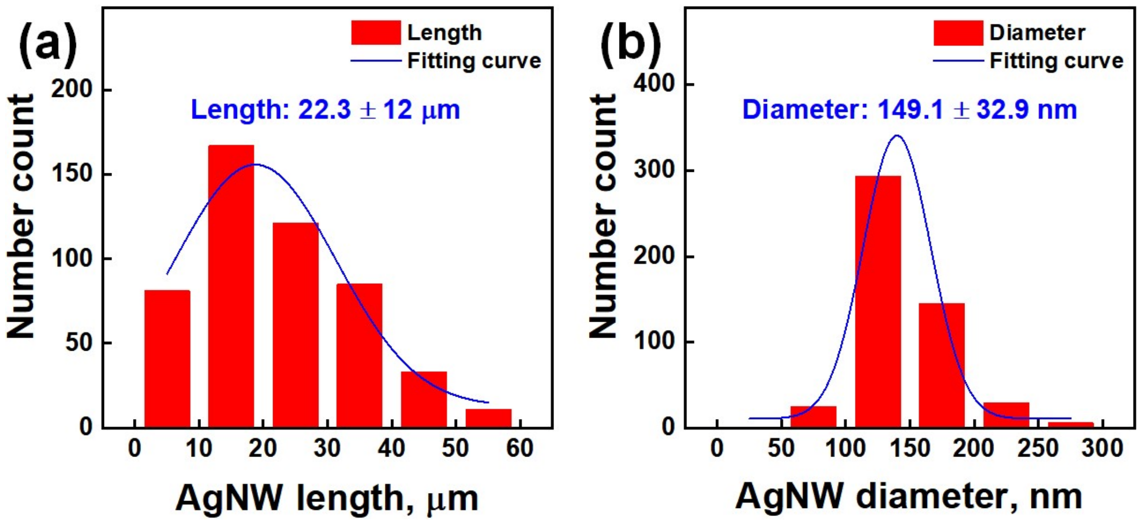

Fig. S4 (a) Length and (b) diameter distributions of the synthesized AgNWs.

In addition to strain sensor applications, various functional silver nanostructures such as nanowires,[S1–S3] nanoparticles,[S4–S7] and nanosheets[S8] have been widely used for various purposes in diverse fields: electromagnetic interference shielding devices,[S1,S2] electrocardiogram electrodes,[S3] antimicrobial applications,[S4–S7] and piezoresistive pressure sensors.[S8]

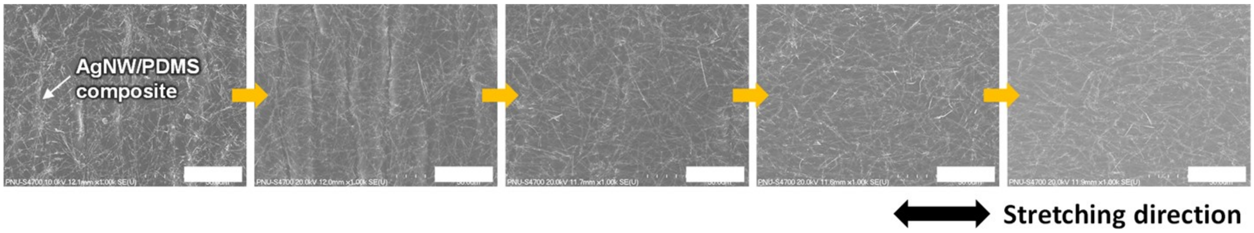

Fig. S5 Sequential SEM images showing the strain-dependent morphological evolution of the AgNW network of the reference composite sensor without a kirigami cut design (scale bars: 30 μm).

The top-view SEM images in Fig. S5 show the AgNW/PDMS composite after being subjected to some pre-stretching cycles. The buckles on the surface of the AgNW/PDMS composite might be induced in the process of releasing strains caused by mechanical instability of the bilayer composite substrate comprising two layers with different mechanical stiffness (i.e., AgNW/PDMS composite layer and pure PDMS layer).[S9–S11]

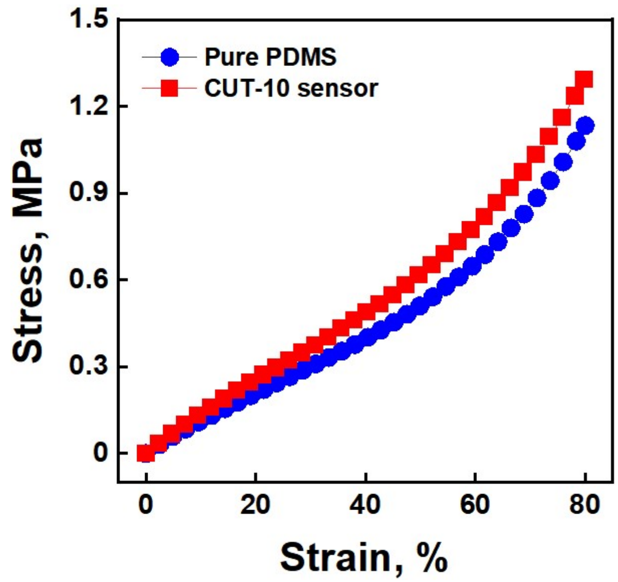

Fig. S6 Stress-strain curves of the CUT-10 strain sensor and pure PDMS sheet.

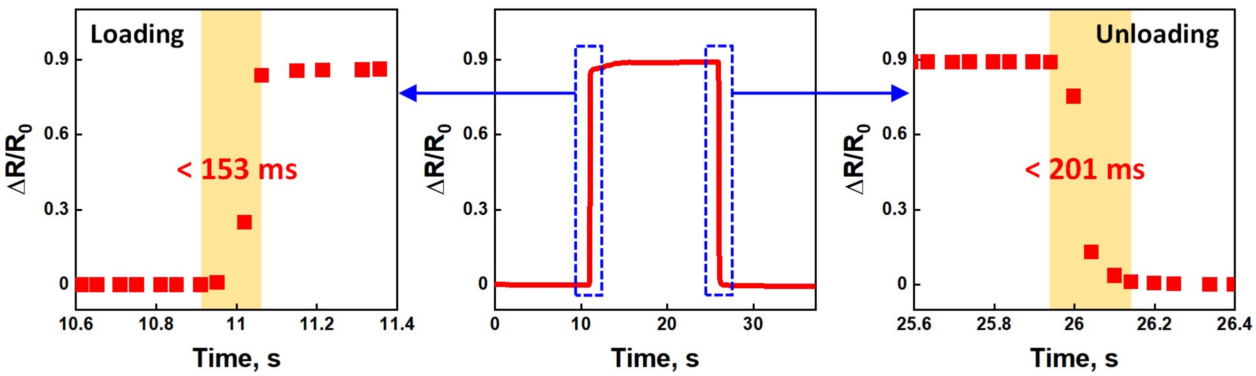

Fig. S7 Time response of the CUT-10 strain sensor when loading and unloading 3% strain at a speed of 600 mm/min.

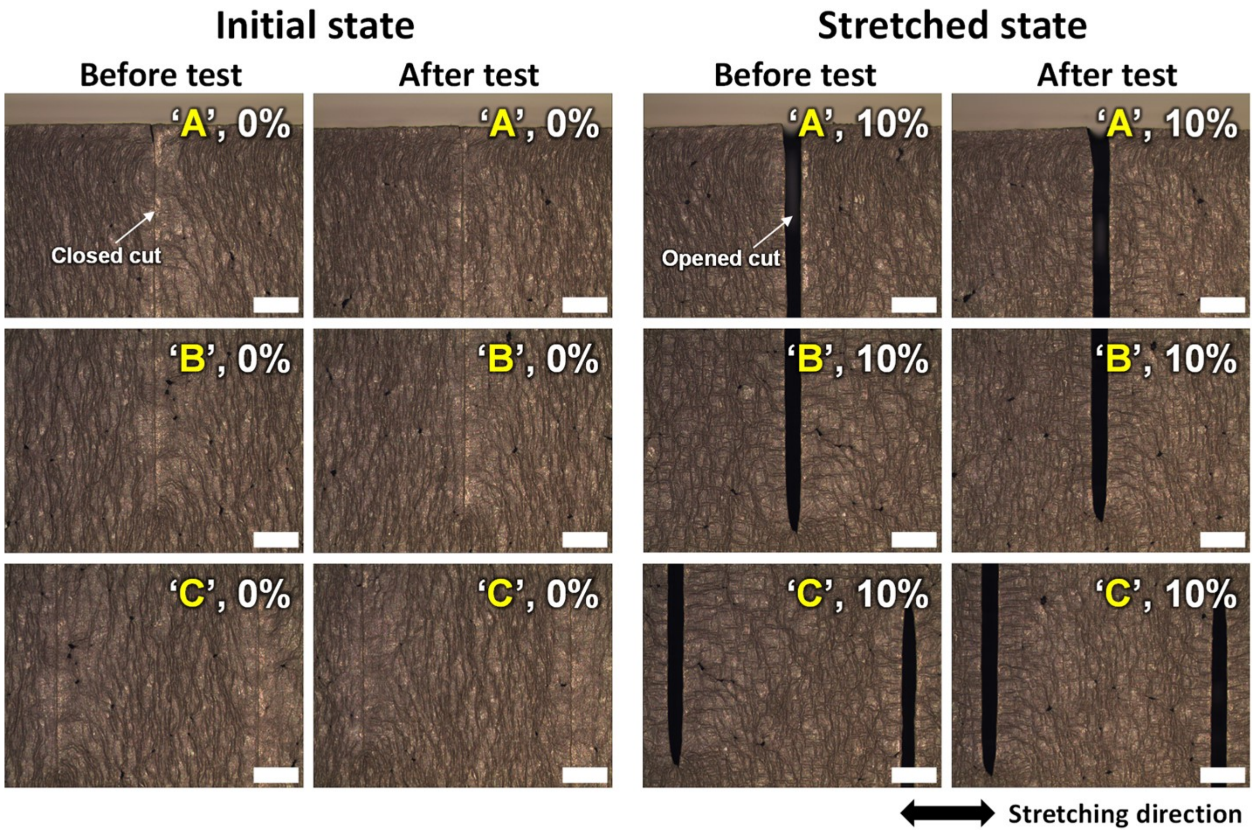

Fig. S8 Top-view microscope images of the CUT-10 strain sensor (a) before and (b) after 1000 stretching cycles at 80% strain (scale bars: 200 μm).

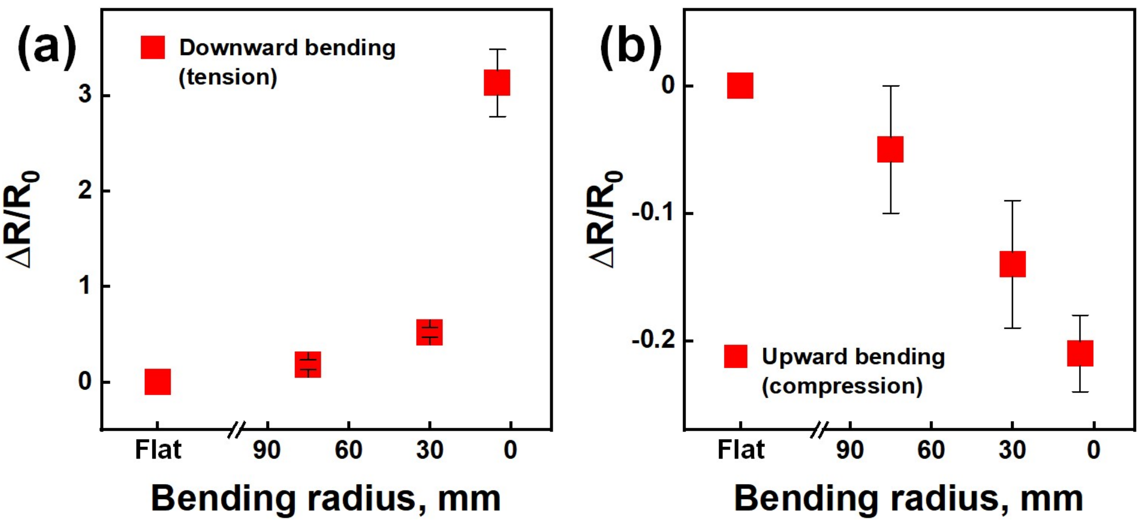

Fig. S9 Relative change in resistance ($\Delta R/R_0$) of the CUT-10 strain sensor under (a) outward and (b) inward bending deformations at various bending radii.

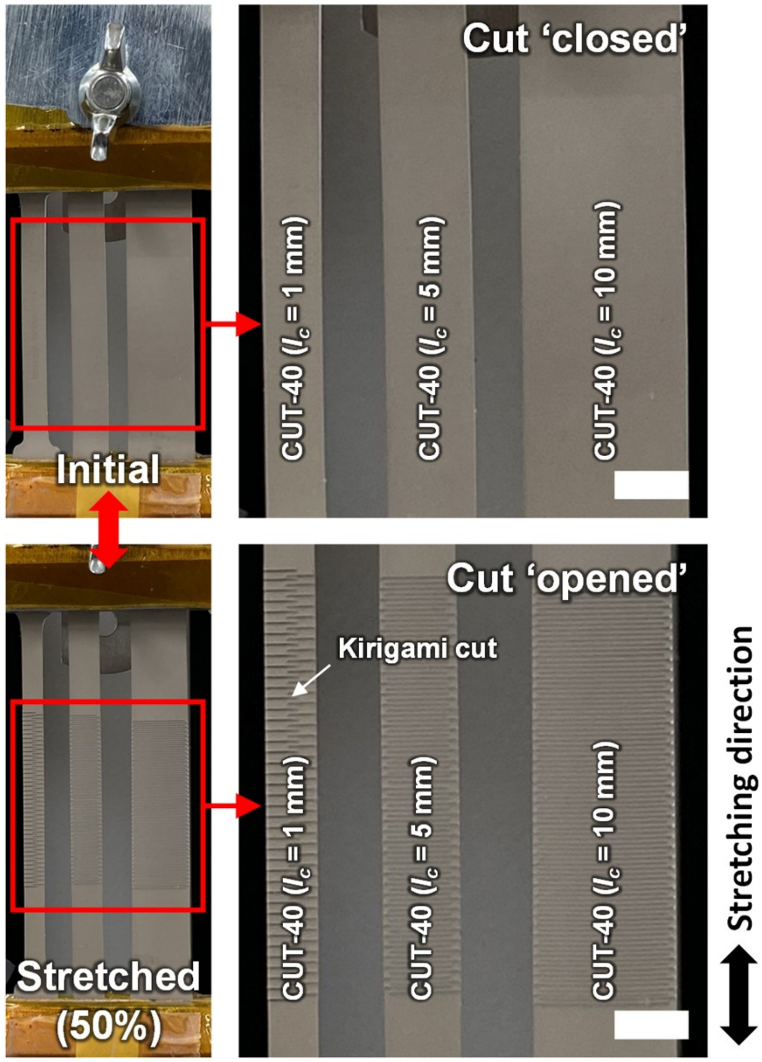

Fig. S10 Digital photographs of the CUT-40 strain sensors with different overlap cut lengths (l_c = 1, 5, and 10 mm) in the initial and 50%-stretched states (scale bars: 5 mm).

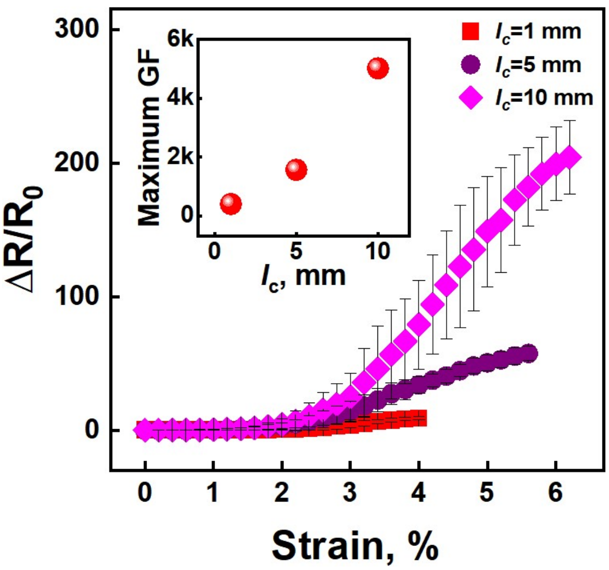

Fig. S11 $\Delta R/R_0$ curves for the first stretching phase of the CUT-40 strain sensors with different overlap cut lengths (l_c = 1, 5, and 10 mm) (inset: maximum gauge factors (GFs) of the devices in the first stretching phase.).

Table S1 Quantitative sensor responses of each CUT strain sensor model in the first stretching phase.

	ε (%)	GF	R^2
CUT-10	0–0.6	2.8	0.955
	0.6–1.2	13.3	0.951
	1.2–3	63.1	0.992
CUT-20	0–0.6	4.3	0.938
	0.6–1.2	24.1	0.953
	1.2–3.8	134.5	0.994
CUT-30	0–0.6	3.5	0.946
	0.6–1.2	17	0.955
	1.2–3.8	280.5	0.983
CUT-40	0–0.6	2.3	0.981
	0.6–1.6	18.6	0.903
	1.6–4	400.2	0.958

Table S2 Quantitative sensor responses of the CUT-40 strain sensors with different cut lengths (lc) in the first stretching phase.

	ε (%)	GF	R^2
l_c = 1 mm	0–0.6	2.3	0.981
	0.6–1.6	18.6	0.903
	1.6–4	400.2	0.958
l_c = 5 mm	0–0.6	13.7	0.901
	0.6–1.6	141.5	0.926
	1.6–5.6	1562	0.987
l_c = 10 mm	0–0.6	18.7	0.926
	0.6–1.6	160.2	0.923
	1.6–6.2	5013.1	0.969

Table S3 Comparison of sensitivity enhancement techniques for CEC-based strain sensors.

Strategy	Stretchability	Sensitivity (GF @ strain)	Ref.
Density control of fillers	500%	7 @ 50%	Chen at al. (2016) [13]
	43% 106% 217%	22 @ 0–15% 6.5 @ 0–15% 2.0 @ 0–15%	Kumar et al. (2019) [14]
	30% 90% 110%	47 @ < 30% 19 @ < 90% 8 @ < 110%	Arif et al. (2018) [15]
	80%	2.2 @ 0–40%	Ren et al. (2017) [25]
Hybridization of fillers	300%	0.91 @ 0–100%	Zheng et al. (2018) [17]
	50%	35 @ 0–20%	Kumar et al. (2022) [18]
	100%	6.3 @ 0–40%	Zhou et al. (2020) [20]
	70%	5.96 @ 0–3%	Lan et al. (2019) [26]
	60%	10 @ 0–15%	Nankali et al. (2020) [27]
Structural modification of composites	400%	740 @ 0–150%	Yang et al. (2023) [31]
	210%	20 @ 0–50%	Zhang et al. (2022) [33]
	25%	1.1 @ 0–18%	Li et al. (2017) [34]
	800%	5.8 @ 0–200%	Zhou et al. (2019) [35]
	150%	24.6 @ 0–130%	Kim et al. (2018) [36]
	55%	84.1 @ 0–6%	Zhang et al. (2022) [37]
Structural modification of substrates	68%	4.5 @ 0–25%	Ha et al. (2022) [38]
	50%	926 @ 9.6%	Heo et al. (2017) [39]
Kirigami cut design	80% 80% 80%	63.1 @ 1.2–3% (N_c = 10, l_c = 1 mm) 400.2 @ 1.6–4% (N_c = 40, l_c = 1 mm) 5013.1 @ 1.6–6.2% (N_c = 40, l_c = 10 mm)	This work

References

S1 K. Liu, W. Liu, Y. Duan, K. Zhou, S. Zhang, S. Ni, T. Xu, H. Du, and C. Si, *Adv. Compos. Hybrid Mater.*, 2022, **5**, 1078.
S2 H. Cheng, Y. Pan, Q. Chen, R. Che, G. Zheng, C. Liu, C. Shen, and X. Liu, *Adv. Compos. Hybrid Mater.*, 2021, **4**, 505.
S3 K. Huang, J. Liu, S. Lin, Y. Wu, E. Chen, Z. He, and M. Lei, *Adv. Compos. Hybrid Mater.*, 2022, **5**, 220.
S4 S. K. Kale, G. V. Parishwad, A. S. N. Husainy, and A. S. Patil, *ES Food Agrofor.*, 2021, **3**, 17.
S5 O. M. Atta, S. Manan, M. Ul-Islam, A. A. Q. Ahmed, M. W. Ullah, and G. Yang, *ES Food Agrofor.*, 2021, **6**, 12.
S6 S. R. Prasad, S. B. Teli, J. Ghosh, N. R. Prasad, V. S. Shaikh, G. M. Nazeruddin, A. G. Al-Sehemi, I. Patel, and Y. I. Shaikh, *Eng. Sci.*, 2021, **16**, 90.
S7 T. Wang, Wusigale, D. Kuttappan, M. A. Amalaradjou, Y. Luo, and Y. Luo, *Adv. Compos. Hybrid Mater.*, 2022, **4**, 696.
S8 J. Liu, E. Chen, Y. Wu, H. Yang, K. Huang, G. Chang, X. Pan, K. Huang, Z. He, and M. Lei, *Adv. Compos. Hybrid Mater.*, 2022, **5**, 1196.
S9 J. -Y. Noh, S. -H. Ha, G. R. Jeon, and J. -M. Kim, *Compos. Sci. Technol.*, 2022, **230**, 109738.
S10 M. Amjadi, A. Pichitpajongkit, S. Lee, S. Ryu, and I. Park, *ACS Nano*, 2014, **8**, 5154.
S11 F. Xu and Y. Zhu, *Adv. Mater.*, 2012, **24**, 5117.